SIAM J. SCI. COMPUT.
Vol. 22, No. 4, pp. 1489–1510

A MODIFIED FRACTIONAL STEP METHOD FOR THE ACCURATE APPROXIMATION OF DETONATION WAVES*

CHRISTIANE HELZEL†, RANDALL J. LEVEQUE‡, AND GERALD WARNECKE†

Abstract. The numerical approximation of combustion processes may lead to numerical difficulties, which are caused by different time scales of the transport part and the reactive part of the model equations. Here we consider a modified fractional step method that overcomes this difficulty on standard test problems and allows the use of a mesh width and time step determined by the nonreactive part, without precisely resolving the very small reaction zone. High-resolution Godunov methods are employed and the structure of the Riemann solution is used to determine where burning should occur in each time step. The modification is implemented in the software package CLAWPACK. Numerical results for 1D and 2D detonation waves are shown, including a detonation wave diffracting around a corner.

Key words. combustion, finite volume, fractional step, Godunov methods, stiff source terms

AMS subject classifications. 65M06, 35L65

PII. S1064827599357814

1. Introduction.

We consider hyperbolic systems of conservation laws with source term which arise in the modeling of combustion processes. Here the source term describes a chemical reaction, i.e., a burning process which leads to a production or reduction of physical quantities inside the domain considered. Under appropriate smoothness assumptions the differential form of a system of conservation laws with source term is given as

$$q_t + \sum_{i=1}^{d} f_i(q)_{x_i} = \psi(q), \tag{1.1}$$

where the physical states $q(x,t)$, the fluxes f_i, and the source ψ are vector-valued functions and d is the space dimension.

If the time scale of the ordinary differential equation (ODE) $q_t = \psi(q)$ for the source term is orders of magnitude smaller than the time scale of the homogeneous conservation law $q_t + \sum_{i=1}^{d} f_i(q)_{x_i} = 0$, then the problem is said to be *stiff*. Here we consider a combustion problem, where the chemical reaction, i.e., the burning process, may be much faster than the gas flow.

We restrict our considerations to numerical solutions which are computed by using a fractional step method, in which we alternate between solving the homogeneous conservation law and the ODEs for the reactions. Furthermore, we solve the homogeneous conservation law by using a high-resolution version of the Godunov scheme,

*Received by the editors June 23, 1999; accepted for publication (in revised form) April 21, 2000; published electronically November 8, 2000.

http://www.siam.org/journals/sisc/22-4/35781.html

†Institut für Analysis and Numerik, Otto-von-Guericke Universität Magdeburg, Postfach 4120, 39016 Magdeburg, Germany (christiane.helzel@mathematik.uni-magdeburg.de, gerald.warnecke@mathematik.uni-magdeburg.de). The work of these authors was supported in part by DFG grants Wa 633/7-1, 2 in the priority research programm DANSE and GIF grant I-318-195.06/93.

‡Department of Applied Mathematics and Department of Mathematics, University of Washington, Box 352420, Seattle, WA 98195-2420 (rjl@amath.washington.edu). The work of this author was supported in part by DOE grant DE-FG03-96ER25292 and NSF grants DMS-9505021, DMS-9626645, and DMS-9803442.

which is implemented in CLAWPACK [18]. It is known that the numerical solutions of conservation laws with stiff source terms may be erroneous, for instance, with discontinuities that propagate at the wrong speed and with nonphysical states. These purely numerical problems are caused by the smearing effect of the conservation law solver. A conservative scheme for solving the homogeneous conservation law leads to smeared-out shock profiles while discontinuities are still moving with the correct speed. In a fractional step scheme this smearing effect may lead to an activation of the very fast process described by the source term. This can produce totally nonphysical solutions. Colella, Majda, and Roytburd [11] have observed nonphysical speeds for a simplified combustion problem. LeVeque and Yee [23] have studied incorrect propagation speeds of a contact discontinuity in the numerical solution of an advection equation with a stiff nonlinear source term.

In order to avoid these problems one could use adaptive mesh refinement or front tracking schemes, see, e.g., Bourlioux [9], LeVeque and Shyue [22], Jeltsch and Klingenstein [16]. Using a sufficiently fine mesh it is always possible to avoid nonphysical solutions since the fractional step method is convergent to the relevant solution. Note that a sufficient spatial resolution is as important as a temporal resolution; see [23].

However, resolution of the fine scale is what one really would like to avoid, if one is not interested in the detailed structure of the detonation wave. Therefore some authors, e.g., Pember [25] or Berkenbosch [7] considered the question of whether it is possible to obtain an accurate numerical solution of a stiff hyperbolic system of conservation laws with source term using time and space steps controlled only by the nonstiff part, i.e., without fully resolving the effect of the stiff source term. With such an *underresolved scheme* one would hope to approximate the global solution structure, e.g., the correct propagation speed of a detonation wave.

Note that this approach is not appropriate if one is interested in processes arising on the scale of the reaction zone, i.e., inside the reaction zone, which we do not want to resolve in the stiff case. A correct approximation of pulsating detonation waves or cellular structures can therefore not be obtained by our modified solver. In order to get such results, one has to resolve the reaction zone.

For the combustion problem, the nonphysical numerical solution that is obtained, if the chemical reaction is not resolved on the grid, is a weak detonation wave usually moving with a speed of one mesh cell per time step. Pember [25] postulated that a necessary condition for such a spurious solution to occur in the numerical calculation could be that the temperature of the post detonation state of the approximated spurious weak detonation wave is higher than the ignition temperature. Therefore, this nonphysical numerical solution can be suppressed if the ignition temperature is high enough. In Berkenbosch [7] the dependency of the numerical solution on the ignition temperature is analyzed in much more detail; see also Berkenbosch, Kaasschieter, and Klein [8]. They also show that the critical ignition temperature needed to get an appropriate approximation of the correct strong detonation wave is lower if a high-resolution scheme for the homogeneous conservation law is used in the fractional step scheme. Based on this observation Berkenbosch [7] and Berkenbosch, Kaasschieter, and Klein [8] suggest using a suitable ignition temperature. A similar change of the ignition temperature was also described by Ton; see [28].

Another possibility to approximate shocks as sharp discontinuities (at least in 1D approaches) is supplied by using the Glimm scheme, which was introduced in [14]. This scheme uses the exact values of the Riemann problem at a randomly chosen point inside every mesh cell. The good performance of the Glimm scheme used in

a fractional step approach to solve the reactive Euler equations is demonstrated in Colella, Majda, and Roytburd [11]. A projection step that eliminates intermediate states which are not in equilibrium was introduced by Sjögreen and Engquist [26] and was tested for 1D and 2D problems. The idea of calculating values at randomly chosen points was recently also used by Bao and Jin [2], [3] in a different way. They replaced the ignition temperature by a uniformly distributed random variable inside the interval of the temperature of the completely unburnt state and the completely burnt state.

In Ben-Artzi [4] and Falcovitz and Ben-Artzi [13] the authors considered the approximation of a Chapman–Jouguet (CJ) detonation wave by using an unsplit second order scheme which is based on the solution of generalized Riemann problems. Their scheme was not intended to resolve the stiffness of the problem. Instead it was constructed in a way that should better approximate the coupling between the fluid dynamical and the chemical equations. For the example used in those papers the ignition temperature is above the critical temperature which is needed for a second order fractional step scheme to approximate the correct detonation front. Their numerical results show that the detonation wave is reasonably approximated if an explicit scheme is used to calculate the reduction of unburnt gas, whereas the use of an implicit scheme leads to the unphysical weak detonation wave.

Here we discuss a modification of the fractional step scheme for the approximation of underresolved detonation waves which gives promising numerical resolution for all appropriate ignition temperatures. It turns out that one can get all the information required for this modification from the structure of the Riemann problems occurring in the discretization. We believe that this approach could also give more insight into the numerical problems occurring when solving conservation laws with stiff source terms.

2. The 1D combustion problem.

2.1. The reactive Euler equations. For modeling the combustion process we use the reactive Euler equations as described, for instance, in [12], [15], [20]. We make use of the following basic assumptions. There are only the two chemical states: burnt gas and unburnt gas. The unburnt gas is converted to burnt gas via an irreversible, exothermic chemical reaction described by the function $K(T)$. The reaction rate $K(T)$ depends on the temperature T via an *Arrhenius law* modeled by

$$K(T) = K_0 \exp\left(-E^+/T\right), \tag{2.1}$$

where K_0 is the rate constant and E^+ is the activation energy; see, for instance, Oran and Boris [24]. The reaction rate is negligible for low temperature values and grows exponentially fast if the temperature is high enough. Sometimes this reaction rate is replaced by a discrete *ignition temperature kinetics model* of the form

$$K(T) = \begin{cases} 1/\tau_0 & : \quad T \geq T_{ign}, \\ 0 & : \quad T < T_{ign}, \end{cases} \tag{2.2}$$

where T_{ign} is the ignition temperature and τ_0 is the time scale of the chemical reaction. Note that $1/\tau_0$ roughly corresponds to K_0 in (2.1). In a stiff calculation, where we do not want to resolve the reaction zone, the discrete ignition temperature kinetics model is a reasonable approximation of the Arrhenius law. Therefore, we will first restrict our considerations to this simplified reaction rate. Later we will show that

our modified scheme can also be applied to the more general form of the Arrhenius law (2.1).

The value τ_0 in (2.1) must be seen in relation to the time scale of the convective part of our problem. Further we assume that the burnt and unburnt gases are ideal gases with the same ratio of specific heats γ and temperature $T = p/\rho\mathcal{R}$, where $\mathcal{R}$ is the specific gas constant. Finally we ignore the effects of diffusion. Using all of these assumptions we get the model equations

$$\rho_t + (\rho u)_x = 0 \qquad \text{conservation of mass,} \tag{2.3}$$

$$(\rho u)_t + (\rho u^2 + p)_x = 0 \qquad \text{conservation of momentum,} \tag{2.4}$$

$$E_t + (u(E+p))_x = 0 \qquad \text{conservation of energy,} \tag{2.5}$$

$$(\rho Z)_t + (\rho u Z)_x = -K(T)\rho Z \qquad \text{continuity equation for the unburnt gas,} \tag{2.6}$$

as a combination of the Euler equations with the kinetics model. The variable Z is the mass fraction of unburnt gas, where $Z = 1$ describes the unburnt state and $Z = 0$ the completely burnt state. The other variables are as usual the total density of burnt and unburnt gas ρ, the velocity u, the pressure p, and the total energy E. The total energy is calculated via the equation of state

$$E = \frac{p}{\gamma - 1} + \frac{1}{2}\rho u^2 + q_0 \rho Z, \tag{2.7}$$

where q_0 is the heat release and the term $q_0\rho Z$ is the chemical energy. Note that by using (2.3), (2.6) is equivalent to

$$Z_t + uZ_x = -K(T)Z. \tag{2.8}$$

There are two combustion processes which are associated with the reactive Euler equations, namely, detonations and deflagrations. Here we restrict our considerations to the approximation of detonation processes; see, for instance, Courant and Friedrichs [12], Godlewski and Raviart [15], or Berkenbosch [7] for a characterization of these processes. We will consider the special case of a CJ detonation wave, which is the detonation wave that occurs most frequently in practice.

The solution structure that can be derived from the reactive Euler equations was originally considered by Zel'dovich, von Neumann, and Döring and is therefore called a *ZND structure*. The detonation process is initiated by a shock. Through this shock, pressure, density, and temperature are raised instantaneously. If the temperature of the unburnt gas becomes greater than the ignition temperature, then the combustion is initiated. Through the combustion process, pressure and density are decreased; see Figure 1. For numerical experiments it is useful to start with such an exact ZND structure as initial data. In this case the exact traveling wave solution and especially the exact propagation speed of the detonation wave can be calculated.

We say that the reactive Euler equations for approximating a detonation wave are *stiff* if the reaction zone is small relative to the mesh size $\triangle x$, in which case the ZND structure cannot be resolved on the grid. This is consistent with the characterization of stiffness given in the introduction because the time scale of the chemical reaction τ_0 is proportional to the length of the reaction zone. In this case the time step appropriate for the fluid dynamics is also insufficient to resolve the kinetics.

2.2. Numerical solutions by using the fractional step method. We use a fractional step method to calculate the numerical solution, e.g., we split the calculation

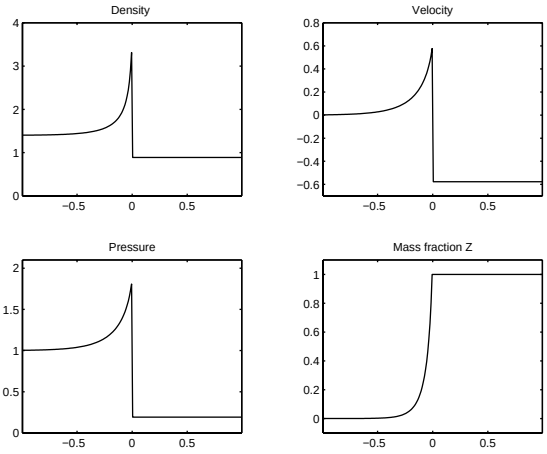

FIG. 1. *ZND structure of a CJ detonation wave.*

of (1.1) into the subproblems

$$q_t + f(q)_x = 0, \tag{2.9}$$

$$q_t = \psi(q) \tag{2.10}$$

and alternate between evolving these numerically. Let $L_{CL}^{\triangle t}$ denote an approximate solution operator of the conservation law (2.9) and $L_{ODE}^{\triangle t}$ be an approximate solution operator of the ODE (2.10), each over a time step of length $\triangle t$. Then the numerical solution at time step t_{n+1} is calculated from the numerical solution at time t_n via the relation

$$Q^{n+1} = L_{ODE}^{\triangle t} L_{CL}^{\triangle t} Q^n.$$

Here, we will restrict our considerations to this "Godunov splitting" scheme, but the results can also be extended to other fractional step methods, e.g., the Strang splitting scheme. See, for instance, LeVeque [20] for more details on fractional step methods. We use a high-resolution version of the Godunov scheme with an exact Riemann solver for solving the system of conservation laws. The solution of the Riemann problem for the nonreactive two-component Euler equations, i.e., the solution of (2.3)–(2.6) with $K(T) = 0$ and piecewise constant initial values, is very similar to the solution of the Riemann problem for the Euler equations. The solution theory of this frequently-used Riemann problem is well known; see, e.g., Smoller [27] or Kröner [17]. This solution consists of constant states separated by three waves, where the 2-wave is always a contact discontinuity. The quantities u and p are Riemann invariants of the 2-wave, thus they are constant across the contact discontinuity. The 1- and the 3-wave are shock or rarefaction waves. Further it is known that the characteristic speed of the contact discontinuity is equal to u. The mass fraction of unburnt gas in the homogeneous part of (2.8) is advected with the speed u, i.e., with the speed of the contact discontinuity. Therefore the mass fraction of unburnt gas in a Riemann problem is equal to Z_l everywhere to the left of the contact discontinuity and equal to Z_r everywhere to the right-hand side of this 2-wave. Different iterative schemes for solving the Riemann problem for the Euler equations were developed, for instance, the Chorin

algorithm [10]. The latter can easily be extended to solving the Riemann problem of the nonreactive two-component Euler equations. It was used in our calculations.

The second step in the fractional step scheme consists in solving the ODE for the source term. The assumption that $K(T)$ is constant is permissible for the ignition temperature kinetics model (2.2). Therefore, the ODE $Z_t = -K(T)Z$ can be solved exactly. We get the solution

$$Z_j^{n+1} = \exp\left(-K(\overline{T}_j^n)\triangle t\right)\overline{Z}_j^n,$$

where $\overline{Z}_j^n$ and $\overline{T}_j^n$ are the values after one time step $\triangle t$ of the conservation law solver. We consider the following test problem of a CJ detonation wave moving with speed one.

Example 1. The initial values consist of totally burnt gas on the left-hand side and totally unburnt gas on the right-hand side. The density, velocity, and pressure of the burnt gas are given by $\rho_b = 1.4$, $u_b = 0$, $p_b = 1$, and $Z_b = 0$. It is then possible to calculate the values for the unburnt state so that the states are connected by a CJ detonation wave moving with speed 1. We find that $\rho_u = 0.887565$, $u_u = -0.577350$, and $p_u = 0.191709$. The mass fraction of unburnt gas is $Z_u = 1$, which means that there is only unburnt gas. Further we can calculate the states within the reaction zone. The other parameters are set to $\gamma = 1.4$, $\mathcal{R} = 1$, and $q_0 = 1$.

For our first set of tests we use the discrete ignition temperature kinetics reaction rate model (2.2). The time scale of the chemical reaction τ_0 as well as the ignition temperature T_{ign} vary in the numerical calculations considered. We consider two values of τ_0 for our experiments: $\tau_0 = 10^{-6}$, in which case the problem is stiff on all grids we consider, and the nonstiff case $\tau_0 = 0.1$. In Figure 1 the ZND structure is shown for the nonstiff case, and these values are also used as initial data. The temperature is increased by the shock. The wave propagates to the right into unburnt gas and the temperature directly behind the fluid dynamical shock is called the *von Neumann temperature*, T_{vN}. The ignition temperature has to be higher than T_u, i.e., higher than the temperature of the unburnt gas, and lower or equal to T_{vN}. In our example the von Neumann temperature is $T_{vN} = 0.545918$ and the temperature of the unburnt gas is $T_u = 0.21598$. Note that the same initial value problem was considered in LeVeque [20] where some preliminary results with this approach were presented.

Now we set $\tau_0 = 10^{-6}$ and $T_{ign} = 0.22$, i.e., the problem is stiff and the temperature is only slightly higher than the temperature of the unburnt gas. In this case the fractional step scheme produces a nonphysical solution, a discontinuity which is propagating with a speed of one mesh cell per time step as mentioned in the introduction; see Figure 2.

This phenomenon has been studied by several authors, see, for instance, [8], [9], [11], [13], and it is well understood that it is caused by the numerical diffusion of the conservation law solver feeding into the fractional step method. For understanding this purely numerical problem we consider one time step using the fractional step method to approximate a detonation wave in a very stiff case, i.e., the reaction zone is much smaller than the width of one mesh cell. For this stiff case the Riemann problem, consisting of totally unburnt gas at the right-hand side and totally burnt gas at the left-hand side, would be a reasonable approximation of the ZND structure. Now we apply one time step of the Godunov scheme to this Riemann problem. The solution structure of the Riemann problem considered is indicated in Figure 3.

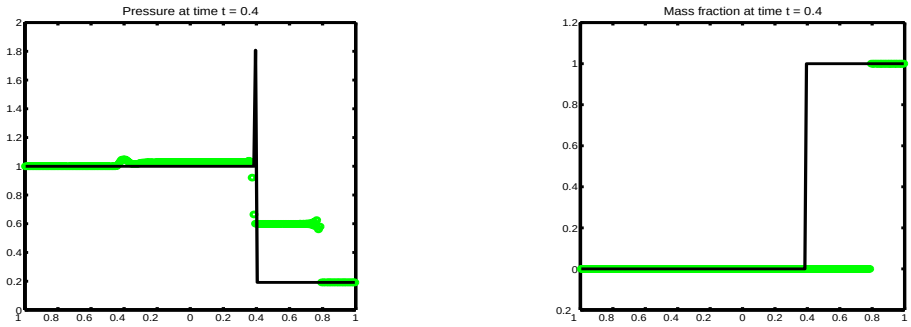

FIG. 2. *Exact* (− − −) *and numerical* (ooo) *solution using the classical fractional step method, with high-resolution Godunov scheme. Parameter values:* $\tau_0 = 10^{-6}$, $T_{ign} = 0.22$, $\triangle x = 0.01$, *and* $\triangle t = 0.005$, *giving a Courant number between* 0.5 *and* 1.

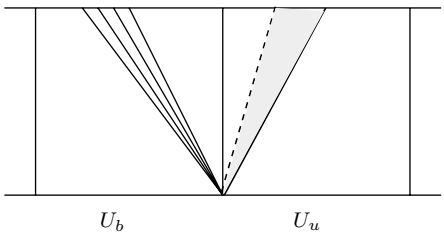

FIG. 3. *Structure of the Riemann solution for the reactive Euler equations. From left to right:* 1*-rarefaction wave,* 2*-contact discontinuity,* 3*-shock; left state: completely burnt gas, right state: unburnt gas.*

The rightmost wave (3-wave) is a shock moving into the unburnt gas. The 2-wave denoted by a dashed line is the contact discontinuity separating burnt gas to the left from initially unburnt gas to the right. However, the shock increases the temperature of the unburnt gas in the region between the 3-wave and 2-wave (the shaded region in Figure 3). The temperature is now greater than T_{ign} and this gas will burn. In the stiff case it burns completely during this time step.

The incorrect propagation speed in the fractional step method arises from the fact that the structure shown in Figure 3 is first averaged over the grid cells to create new piecewise constant states before the reaction terms are applied. As a result the entire grid cell to the right in Figure 3 obtains a single averaged temperature. If this is greater then T_{ign} then *all* the unburnt gas in this cell burns during the reaction step, including the gas to the right of the 3-wave. This causes the interface between burnt and unburnt gas to advance by one full grid cell. See [23] for more details. The closer T_{ign} is to T_u the more likely this is to happen. If T_{ign} is considerably larger than T_u, then in some steps the full cell will burn and in other steps nothing will burn, and the average speed could still come out close to correct. Furthermore, if the ignition temperature is high enough then an unphysical intermediate state (for instance in pressure) lower than the value of the completely burnt state can not be obtained. This has been investigated by Berkenbosch [7]; see also [8].

2.3. Modification of the fractional step method. We have seen that the nonphysical solutions are a consequence of smearing the reaction zone before burning. Using this observation we construct a modification of the fractional step scheme which

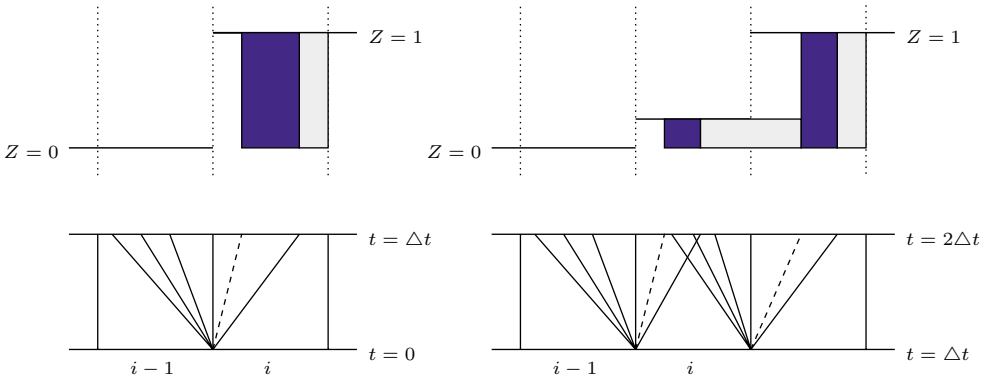

FIG. 4. *Modification of the scheme along the smeared-out reaction front in the stiff case. Left: first time step; right: second time step.*

eliminates those combustion processes which are purely a consequence of the smearing effects. First we consider the stiff case, in which the exact reaction zone is smaller than one mesh cell and the reactions take place very fast.

Again considering the situation which is shown in Figure 3, we should allow a reaction only between the shock and the contact discontinuity in the first time step, because only there do sufficiently high temperature and unburnt gas coexist. The essential idea of our approach is to apply the ODE solver only in the region where burning should occur. In the first time step this is easy, but after one time step we do expect some smearing of the correct shock location and hence a nonphysical "average" temperature in at least one grid cell. Now we want to interpret the cell average in a different way. As shown in Figure 4 the piecewise constant initial values for the second time step contain one mesh cell i, where the mass fraction of unburnt gas Z has a value with $0 < Z < 1$. The average of the temperature in cell i might be higher than the ignition temperature, but more correctly the burnt gas in cell i has a temperature higher than T_{ign} and the unburnt gas has a temperature lower than T_{ign}.

In the stiff case the reaction takes place very fast and during one time step the whole portion of the gas which was heated up by the shock has already burnt. Therefore we interpret the gas flow described by the homogeneous conservation law in the second time step as a transport of the unburnt gas. A reaction can only take place if this unburnt gas is ignited by a shock. This modification is described in Figure 4. The shaded areas indicate the mass fraction of unburnt gas after the transport by the homogeneous conservation law. Only in the dark shaded area a reaction is initiated. We make use of the fact that a rarefaction wave, such as the one generated between cells i and $i + 1$, cannot increase the temperature of the unburnt gas. In consequence there is no reaction to the right of the 3-shock in cell i even though the *average* value of the temperature might be higher than T_{ign}. The solution structure could also consist of a 1-shock and a 3-shock. In this case we allow a reaction between these two waves.

The temperature as well as the pressure can only be increased by a shock. We observe that along the smeared-out reaction front the Riemann problems occurring in each time step for solving the homogeneous conservation law have a 3-shock if the combustion front moves from left to right.

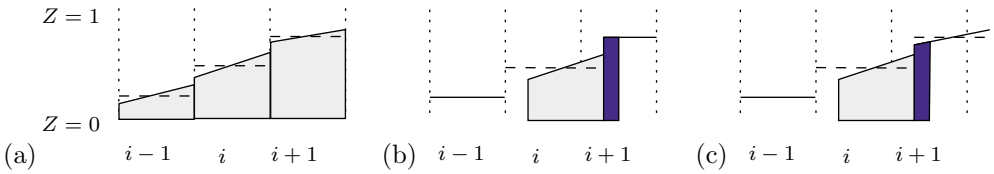

FIG. 5. *Description of the modification using the high-resolution wave propagation algorithm.*

On the other hand, a mesh cell may also lie within the reaction zone. If the temperature in a mesh cell is higher than the ignition temperature and there is still unburnt gas but no shock wave is coming into this mesh cell that will further increase the temperature there, then this cell belongs to the (smeared-out) reaction zone. In this case we allow the burning process in the whole mesh cell; i.e., we use the classical fractional step method.

For our example of a CJ detonation wave moving from the left- to the right-hand side, we can easily determine whether a mesh cell belongs to the smeared-out shock or to the reaction zone and, hence, whether the burning process in the stiff case should take place between shock and contact discontinuity, or in the whole mesh cell by only considering the 3-wave. If the 3-wave is a shock, then we allow the burning process only between the shock and contact discontinuity, and if the 3-wave is a rarefaction wave, then we allow the burning process in the whole mesh cell.

By using a second order finite volume scheme, sharper results can be obtained in which discontinuities are smeared-out over fewer mesh cells than when using first order schemes. Nevertheless, in combination with a fractional step scheme, the same numerical problems occur for both first and second order approximations of the conservation laws if the source term is not treated carefully. Note that the numerical results which are shown in Figure 2 were calculated with a high-resolution Godunov scheme to approximate the convective part. The same nonphysical solution would be obtained using the first order Godunov scheme. For our improved numerical calculations we have combined the high-resolution wave propagation algorithm from CLAWPACK, which is described in LeVeque [21], with the modification of the fractional step scheme described above.

The high-resolution method is based on using piecewise linear reconstruction in place of piecewise constant functions. Slopes are chosen based on nearby solution values, and limiters are applied to avoid spurious oscillations. For all calculations shown in this paper we used the monotonized-centered limiter, proposed by van Leer [29] and given explicitly in [21] in the context of CLAWPACK. Other standard limiters, e.g., minmod or superbee, which are also available in CLAWPACK were also tested and gave comparable results. Figure 5(a) shows the piecewise linear reconstruction of Z in three grid cells. From the structure of the Riemann problem we know that discontinuities in Z are propagated at the speed of the contact discontinuity. In the high-resolution method each piecewise linear structure is propagated at the local fluid speed and then averaged onto the grid; see [21]. With combustion, we again wish to apply burning only to the unburnt gas lying between a shock and contact where the temperature has been raised above the ignition temperature. This is illustrated in Figure 5(b) and (c) for the case where such a shock arises from the Riemann problem between cells i and $i+1$ and moves into cell $i+1$ at a speed greater than the contact speed. Hence, it is the unburnt gas initially in cell $i+1$ which now burns, as indicated by the dark shaded region in each figure. In Figure 5(b) we simply use the cell average

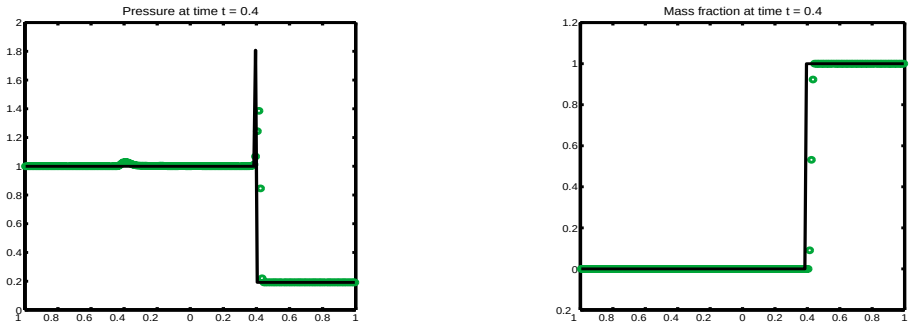

FIG. 6. *Exact and numerical solution using the modification, with high-resolution Godunov scheme. Parameter values:* $\tau_0 = 10^{-6}$ *and* $T_{ign} = 0.22$, $\triangle x = 0.01$, $\triangle t = 0.005$ *giving a Courant number between* 0.5 *and* 1.

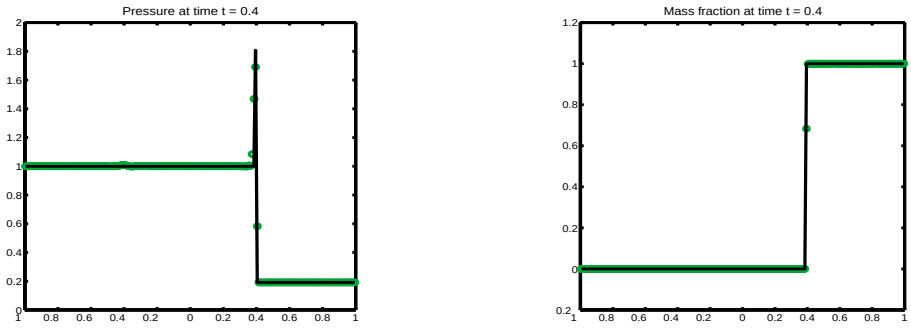

FIG. 7. *Exact and numerical solution using the modification, with high-resolution Godunov scheme. Parameter values:* $\tau_0 = 10^{-6}$ *and* $T_{ign} = 0.54$, $\triangle x = 0.01$, $\triangle t = 0.005$ *giving a Courant number between* 0.5 *and* 1.

Z_{i+1} to determine how much gas burns. This is easier to implement than the more accurate procedure indicated in Figure 5(c), where the piecewise linear structure in cell $i + 1$ is used to determine the amount that burns. Both have been tested in one dimension but we have found very little difference in the observed accuracy. Consequently, we have used the simpler approach of Figure 5(b) in the 2D extension presented below.

Figure 6 shows the numerical solution of the stiff problem with low ignition temperature using the modification which was described above. One should compare with Figure 2 where the same problem was solved by using the classical fractional step method. In Figure 7 the stiff problem was solved with our modification for a case with a higher ignition temperature, near the von Neumann temperature, in order to show that we get a good approximation of the detonation wave for all possible ignition temperatures.

In the nonstiff case the fractional step method gives a good approximation of the detonation wave, since for this case the two time scales fit together; see LeVeque [20] for a numerical calculation. This is consistent with our modification of the stiff case in the following sense. In the nonstiff case most of the mesh cells with $0 < Z < 1$ belong to the reaction zone and therefore a reaction should take

TABLE 1

Numerical propagation speed, calculated taking (2.11)*, using the classical fractional step method* ($S_{fs,1}$ *or* $S_{fs,2}$) *and the modified method* ($S_{mod,1}$ *or* $S_{mod,2}$) *with first-order and high-resolution versions of the Godunov scheme for different ignition temperatures* (T_{ign}) *and different time scales* τ_0*. The numerical propagation speed is given for the time* $t = 0.4$*. For all calculations we used the mesh width* $\triangle x = 0.01$ *and a time step* $\triangle t = 0.005$ *giving a Courant number between* 0.5 *and* 1*.*

	τ_0	T_{ign}	$S^{0.4}_{fs,1}$	$S^{0.4}_{mod,1}$	$S^{0.4}_{fs,2}$	$S^{0.4}_{mod,2}$
	0.1	0.22	1.052262	1.045323	1.052892	1.044059
Nonstiff	0.1	0.30	1.038623	1.032534	1.047261	1.042274
	0.1	0.40	1.029742	1.029659	1.039676	1.039266
	0.1	0.54	0.985936	0.985932	1.009614	1.009614
	10^{-6}	0.22	2.025000	1.069491	2.000000	1.086376
Stiff	10^{-6}	0.30	1.150000	1.059374	1.125029	1.083180
	10^{-6}	0.40	1.078079	1.043682	1.102789	1.052685
	10^{-6}	0.54	1.025647	1.004062	1.056581	1.007961

place in the whole mesh cell. Now, in contrast to the stiff case, the gas that was heated by the shock did not entirely burn in one time step. Note that this was our main motivation for the modification along the smeared-out reaction front in the stiff case. Therefore, in the nonstiff case we do not restrict a reaction to the region between the shock and contact discontinuity only. Only in the mesh cell where the totally unburnt gas is first heated up by a shock do we need to make an exception. There the reaction should be restricted to the area behind the shock because only there we have a sufficiently high temperature. The numerical results which where obtained with this modification are very similar to those obtained by the classical fractional step method, which is already adequate for the nonstiff case, as seen in Table 1. Note that the approximation of the nonstiff case is also consistent with the transition between the stiff and the nonstiff method which is described below.

Table 1 contains different values for the numerical propagation speed $S^{n\triangle t}$ of the mass fraction of unburnt gas calculated by the formula

$$S^{n\triangle t} = \frac{\triangle x}{n\triangle t} \cdot \sum_{i=-\infty}^{\infty} (Z_i^0 - Z_i^n). \tag{2.11}$$

$S^{n\triangle t}$ is the averaged numerical propagation speed of the detonation wave at time $n\triangle t$, which was calculated via an approximation of the equal area rule; see Berkenbosch [7]. Both a nonstiff and a stiff case are considered with different values of T_{ign}. The correct value of the propagation speed is equal to one in all cases. The index of S in Table 1 further specifies the numerical scheme which was used for the calculation as well as the order. All values of the numerical propagation speed are given for the time $n\triangle t = 0.4$, which corresponds to the time step of the numerical approximations shown in Figure 2 as well as Figures 6 and 7.

Table 1 shows that the classical fractional step scheme gives a good approximation of the stiff problem if the ignition temperature T_{ign} is high enough. This was studied by Berkenbosch in [7] and Berkenbosch, Kaasschieter, and Klein in [8]. With the modified fractional step scheme we always get a more accurate approximation of the shock speed and maintain reasonable accuracy even in the stiff case.

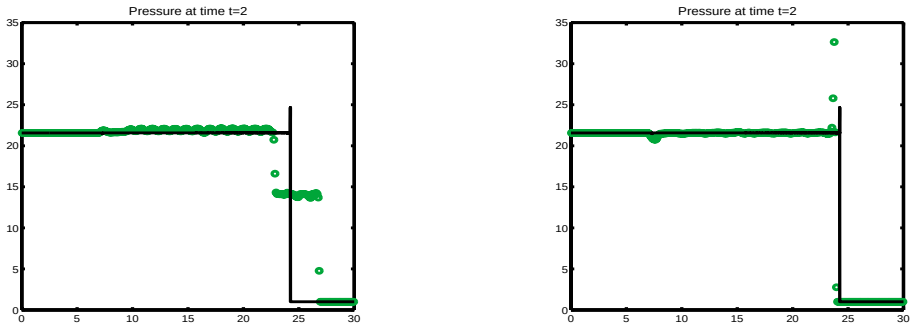

FIG. 8. *Resolved* (− − −) *and underresolved* (ooo) *approximation of the pressure for Example 2. For the resolved calculation we used the mesh width* $\triangle x = 0.0025$*, and for the underresolved calculation we used* $\triangle x = 0.1$*. The classical fractional step scheme gives an unphysical solution (left); the modified fractional step scheme gives an accurate approximation (right).*

In our next example we apply our modified fractional step scheme to the approximation of a stiff detonation wave for which the reaction is modeled by the Arrhenius law (2.1).

Example 2. We consider the reactive Euler equations with the reaction rate law (2.1). The unburnt state is given by $\rho_u = 1$, $u_u = 0$, $p_u = 1$. For the heat release, we used the value $q_0 = 25$ and the activation energy is set to $E^+ = 25$. Furthermore, the ratio of specific heats is set to $\gamma = 1.4$. The unburnt state is connected to the burnt state by a CJ detonation wave. The physical quantities of the completely burnt state are $\rho_b = 1.6812$, $u_b = 2.8867$, $p_b = 21.5672$. The CJ detonation wave has the speed $s_{CJ} = 7.1247$. Initially the discontinuity is located at the point $x = 10$. We use the rate constant $K_0 = 164180$.

Figure 8 shows numerical results of the pressure for underresolved calculations of the detonation wave described in Example 2. The solid line is the reference solution which was calculated on a very fine mesh. Our modified fractional step scheme, which can be applied in the same way as described for the ignition temperature kinetics model, approximates the correct propagation speed of the detonation wave, whereas the usual fractional step scheme again leads to an unphysical weak detonation wave followed by a nonreactive shock.

In order to approximate the transition between the stiff and the nonstiff case on those mesh cells which approximate the smeared-out leading shock of a detonation wave in an appropriate way, we limit the amount of the mass fraction of unburnt gas, which is converted to burnt gas during one time step, from above by $(\triangle Z_i)_{max} = \text{area } Z_i$, where Z_i is the cell average of the mass fraction of unburnt gas and area specifies the part of the mesh cell, where the source term should be applied in a stiff calculation. In the 1D case this part of the mesh cell is given by $\text{area} = \frac{(s-c)\triangle t}{\triangle x}$, where s is the speed of the shock and c is the propagation speed of the contact discontinuity. This implies that along the smeared-out leading shock of a detonation wave, *at most* the whole mass fraction of unburnt gas between shock and contact discontinuity would completely burn. In the nonstiff case the reduction of the mass fraction of unburnt gas due to the ODE for the source term equation applied to the whole cell average will in general be less than $(\triangle Z_i)_{max}$, and our modified fractional step scheme automatically switches to the classical fractional step scheme along the smeared-out leading shock of a detonation wave. The same criteria can be applied to calcula-

tions which use the Arrhenius law (2.1). However, for this reaction rate equation the reaction rate and also the length of the reaction zone depends on the temperature. Therefore, especially in multidimensional examples, the problem can include stiff and nonstiff regions depending on the temperature. We will consider such a problem in section 3.

3. The 2D combustion problem. Now we consider the modification of the scheme for 2D reactive Euler equations, i.e., for the system of equations

$$\rho_t + (\rho u)_x + (\rho v)_y = 0, \tag{3.1}$$

$$(\rho u)_t + \left(\rho u^2 + p\right)_x + (\rho uv)_y = 0, \tag{3.2}$$

$$(\rho v)_t + (\rho uv)_x + \left(\rho v^2 + p\right)_y = 0, \tag{3.3}$$

$$E_t + (u(E+p))_x + (v(E+p))_y = 0, \tag{3.4}$$

$$(\rho Z)_t + (\rho uZ)_x + (\rho vZ)_y = -\rho K(T)Z. \tag{3.5}$$

Here u is the velocity of the gas in x-direction and v is the y-component of the velocity. The equation of state is in the 2D case

$$E = \frac{p}{\gamma - 1} + \frac{1}{2}\rho(u^2 + v^2) + q_0\rho Z.$$

Again we want to use a fractional step scheme for approximating the solution. As in the 1D case we have to apply a modification in order to avoid both nonphysical propagation speeds of the combustion front and wrong intermediate states. For the solution of the homogeneous conservation law we used the high-resolution version of the Godunov scheme implemented in CLAWPACK [18]. The method is based on solving 1D Riemann problems at each cell boundary as well as taking transverse directions into consideration. The part of the flux across a cell boundary which is propagated in the transverse direction is calculated via the tangential Riemann problem based on a Roe linearization; see LeVeque [21]. This improves the stability and accuracy of the scheme.

3.1. Modification of the 2D fractional step method. As we have already mentioned, the 2D version of the Godunov scheme is based on solving 1D Riemann problems in the x- as well as in the y-direction. Therefore, we can use the same modification as in the 1D case; i.e., in the stiff case along the reaction front a reaction will only be possible between the shock and contact discontinuity. This modification is indicated in Figure 9, where we assume the case of a 3-shock.

Now we also want to consider the influence of the transverse propagation. This means that parts of the shaded areas in Figure 9 are propagated into other mesh cells. Here we only want to consider the propagation in the y-direction of the reaction area calculated by a Riemann problem in x-direction. From the transverse Riemann solver we can get a decomposition of each wave into a linear combination of eigenvectors of the Jacobian matrix of the flux functions in the tangential direction. These subwaves are moving upwards or downwards with the speeds μ^i corresponding to the eigenvalues of the Jacobian matrix of the form $\mu^1 = v - c$, $\mu^2 = v$, $\mu^3 = v + c$; see [21].

The most accurate possibility for calculating the transverse propagation of the area where a reaction is supposed to take place would require calculating the temperature for all the subwaves corresponding to the area behind a shock along the reaction zone. If the temperature is higher than the ignition temperature, then the

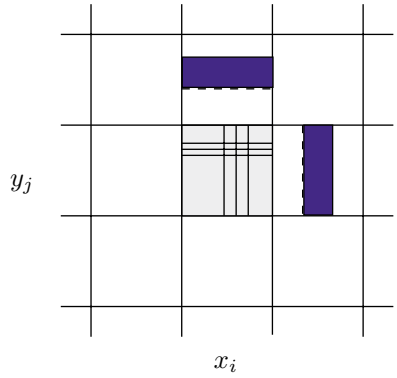

FIG. 9. *Structure of the modification of the normal Riemann problem in x direction between the states $q(x_i, y_j)$ and $q(x_{i+1}, y_j)$ as well as for the Riemann problem in y direction between the states $q(x_i, y_j)$ and $q(x_i, y_{j+1})$ used in the stiff case.*

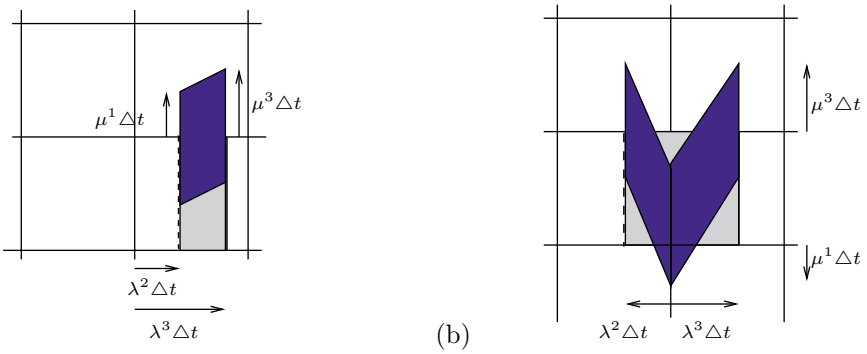

FIG. 10. *Two different possibilities for the transverse modification. The dark shaded regions are the cell portions where a reaction takes place for a Riemann problem in the x-direction with transverse modification.*

area between the shock and contact discontinuity should be propagated in the transverse direction. Such a modification would be quite expensive. For the transverse propagation, it is also not necessary to decouple every wave separately. Instead of decoupling each wave, only the left- and right-going flux differences have to be considered. Therefore, we have used the simplified transverse propagation of cell areas where a reaction takes place as indicated in Figure 10 which only uses the transverse speeds μ^1 and μ^3. If both of these eigenvalues have the same sign, then the area which is propagated in the y direction is equal to the trapezoid with a height equal to the distance between shock and contact discontinuity and the sides $|\mu^1 \triangle t|$ and $|\mu^3 \triangle t|$. This is shown in Figure 10(a) for the case where all eigenvalues are positive. In the case where $\mu^1 < 0$ and $\mu^3 > 0$, we would have a triangular portion corresponding to μ^1, which is moving into the cell below, and another triangular portion moving into the cell above, which corresponds to the eigenvalue μ^3. Figure 10(b) shows yet another possibility: the transverse propagation of the reaction area consisting of a left-going contact discontinuity and a right-going 3-shock assuming also that the eigenvalues μ^1 and μ^3 have different signs.

3.2. Approximation of a radialsymmetric CJ detonation wave. We restrict our considerations to the stiff case where the fractional step scheme may have numerical problems. First we want to note that also in the 2D case the usual fractional step scheme without modification leads to a good approximation if the ignition temperature is high enough. This was observed by Berkenbosch, Kaasschieter, and Klein [8] for 1D and 2D combustion waves.

Example 3. For our numerical computations we consider a radially symmetric CJ detonation wave. The initial values consist of totally burnt gas inside of a circle with radius 0.3 and totally unburnt gas everywhere outside of this circle. Furthermore, the unburnt and burnt states are chosen in a way analogous to the 1D case, i.e., $\rho_b = 1.4$, $\rho_u = 0.887565$, $p_b = 1$, $p_u = 0.191709$, $Z_b = 0$, $Z_u = 1$, $u_b = 0$, $u_u = -0.577350\cos\alpha$, $v_b = 0$, $v_u = -0.577350\sin\alpha$, where α is the angle in polar coordinates. The ignition temperature is set to $T_{ign} = 0.26$.

For this radially symmetric problem it is possible to get more insight into the structure of the solution by comparing the solution calculated with a 2D algorithm and the numerical solution of the 1D system of reactive Euler equations with an additional source term for the radial symmetry. The 1D reactive Euler equations for a radially symmetric problem are

$$\rho_t + (\rho\hat{u})_r = -\frac{1}{r}\rho\hat{u},$$

$$(\rho\hat{u})_t + (\rho\hat{u}^2 + p)_r = -\frac{1}{r}\rho\hat{u}^2,$$

$$E_t + (\hat{u}(E+p))_r = -\frac{1}{r}\hat{u}(E+p),$$

$$Z_t + \hat{u}Z_r = -K(T)Z,$$

where $\hat{u} = u\cos(\alpha) + v\sin(\alpha)$ is the speed in radial direction and $r = \sqrt{x^2 + y^2}$ is the distance from the center. Now we can use the 1D fractional step scheme with the modification for the stiff source term to get an approximation along any radial slice of the 2D combustion wave. The 1D system is solved on a very fine grid ($\triangle x = 0.00025$) so that the numerical solution is assumed to be an accurate approximation of the exact solution. The numerical solutions of the 1D reference problem are plotted as solid lines in Figures 14–16. The scatter plots of the 2D solutions are obtained by plotting the value on each mesh cell as a function of r, i.e. the distance to the center of symmetry.

In the 2D case we have the additional effect that also the gas flow ahead of the combustion front increases the temperature slightly. For simplicity, we are not interested in this effect for the moment. Therefore, we have to choose the ignition temperature higher than the temperature occurring just ahead of the combustion front during the time interval considered.

Figures 11 and 12 as well as the scatter plots Figures 14 and 15 show the numerical calculations at different time steps obtained using the modified fractional step scheme. Here the combustion front moves with the correct speed and, furthermore, the circular geometry is resolved well on the grid.

For contrast, in Figure 13 contour plots of the pressure and mass fraction of unburnt gas are shown, calculated by using the classical fractional step scheme at the

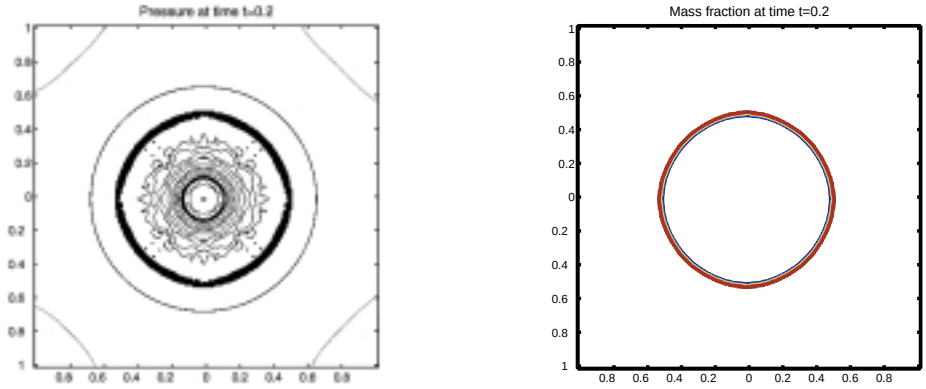

FIG. 11. *Contour plot of pressure and mass fraction of unburnt gas at time* $t = 0.2$ *using the modification with high-resolution Godunov scheme,* $T_{ign} = 0.26$, $\tau_0 = 10^{-6}$, $\triangle x = \triangle y = 0.01$, $CFL \leq 0.75$.

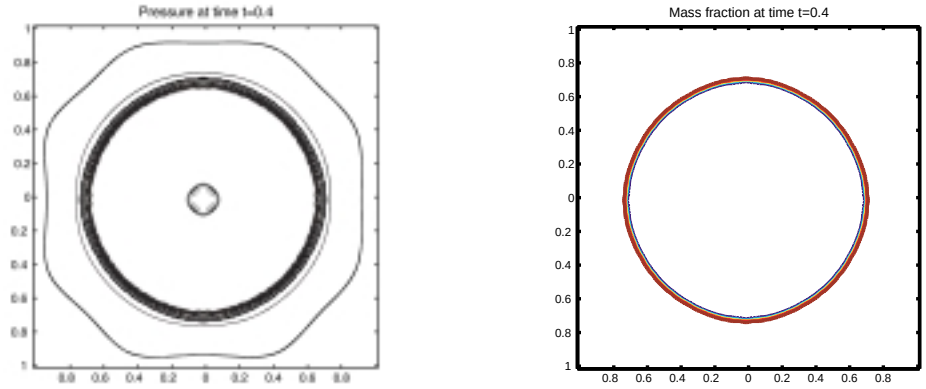

FIG. 12. *Contour plot of pressure and mass fraction of unburnt gas at time* $t = 0.4$ *using the modification with high-resolution Godunov scheme,* $T_{ign} = 0.26$, $\tau_0 = 10^{-6}$, $\triangle x = \triangle y = 0.01$, $CFL \leq 0.75$.

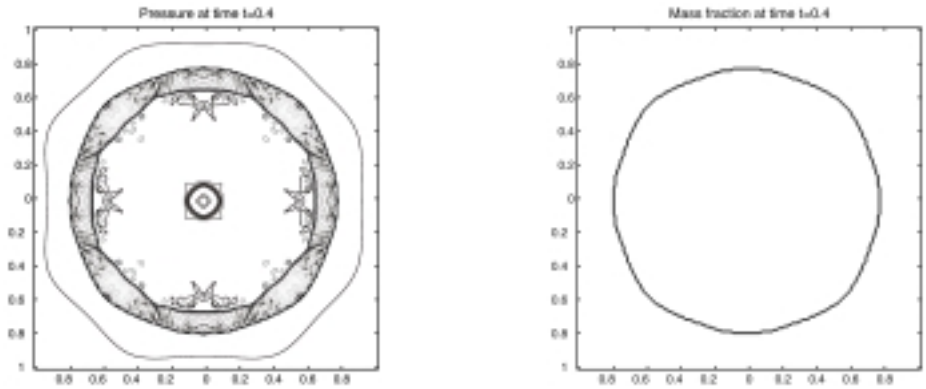

FIG. 13. *Contour plot of pressure and mass fraction of unburnt gas at time* $t = 0.4$ *using the classical fractional step method with high-resolution Godunov scheme,* $T_{ign} = 0.26$, $\tau_0 = 10^{-6}$, $\triangle x = \triangle y = 0.01$, $CFL \leq 0.75$.

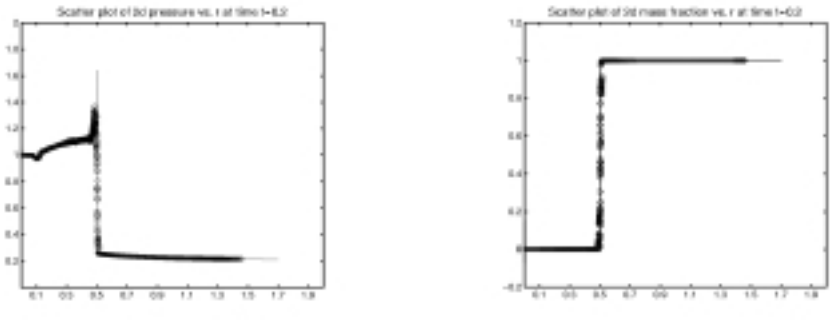

FIG. 14. *Scatter plot of pressure and mass fraction of unburnt gas vs. radius r at time* $t = 0.2$ *using the 2D modification with high-resolution Godunov scheme;* $\triangle x = \triangle y = 0.01$, $\triangle t = 0.005$, $\tau_0 = 10^{-6}$, $T_{ign} = 0.26$.

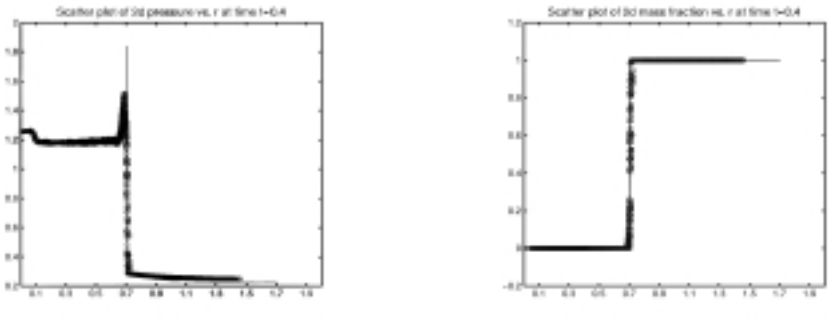

FIG. 15. *Scatter plot of pressure and mass fraction of unburnt gas vs. radius r at time* $t = 0.4$ *using the 2D modification with high-resolution Godunov scheme;* $\triangle x = \triangle y = 0.01$, $\triangle t = 0.005$, $\tau_0 = 10^{-6}$, $T_{ign} = 0.26$.

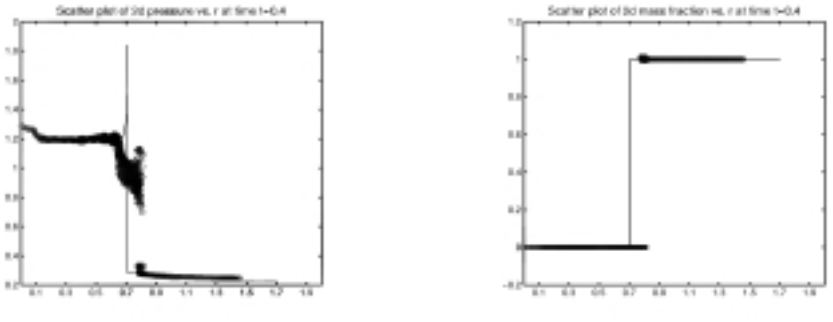

FIG. 16. *Scatter plot of pressure and mass fraction of unburnt gas vs. radius r using the classical fractional step method with high-resolution Godunov scheme;* $\triangle x = \triangle y = 0.01$, $\triangle t = 0.005$, $\tau_0 = 10^{-6}$, $T_{ign} = 0.26$.

later time. The scatter plots in Figure 16 show that the combustion front moves too fast and there is an unphysical intermediate state for the pressure. Moreover, the front does not remain circular.

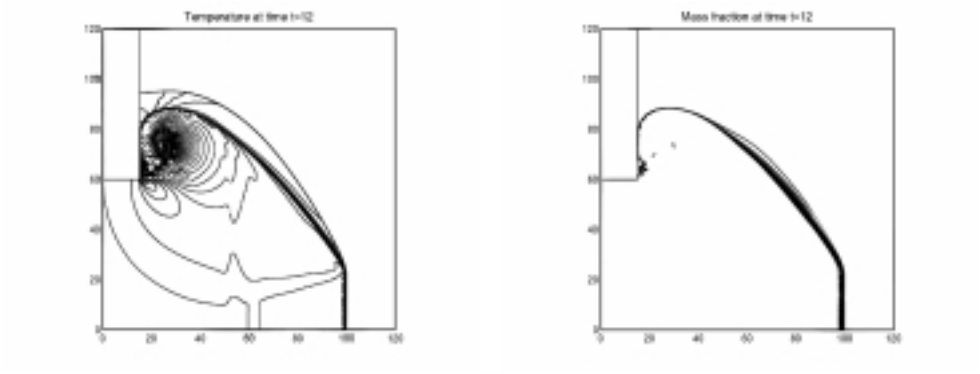

(a) (b)

FIG. 17. *CJ detonation wave defracting around a corner. Resolved adaptive mesh refinement calculation of temperature and mass fraction of unburnt gas.*

TABLE 2

Error, i.e. difference between radial symmetric $1D$ *reference solution and the solution calculated with the* $2D$ *modified fractional step scheme in normal and tangential direction, in* L_1*-norm and experimental order of convergence (EOC) for the* $2D$ *modification using the high-resolution Godunov scheme;* $\tau_0 = 10^{-6}$, $T_{ign} = 0.26$, $t = 0.4$.

$\triangle x = \triangle y$	$\triangle t$	$\| \Delta\rho \|$	$\| \Delta(\rho u) \|$	$\| \Delta E \|$	$\| \Delta Z \|$
0.04	0.02	0.09481	0.05941	0.20250	0.10190
0.02	0.01	0.06477	0.03847	0.14550	0.04795
EOC		0.55	0.63	0.48	1.09
0.01	0.005	0.04258	0.02927	0.09877	0.02150
EOC		0.61	0.39	0.56	1.16
0.005	0.0025	0.02773	0.01945	0.06395	0.01221
EOC		0.62	0.59	0.63	0.82

Finally, Table 2 shows some numerical order of convergence results. For the numerical approximation of this discontinuous solution the expected order of convergence is between 0.5 and 1; see [19]. With our modified fractional step scheme we could achieve such a convergence order without resolving the reaction zone. Although our numerical solution shows the typical von Neumann peak behind the shock front, we get a relatively large error in the region which approximates the very small reaction zone. This might be a reason why the experimental order of convergence for the variables which contain a peak is lower than the order of convergence for the mass fraction of unburnt gas, which in the stiff case only contains a discontinuity.

The transition between the stiff and the nonstiff case is done in a manner analogous to what was described for the 1D case in section 2.3. Now the maximal rate of reduction (area) of the mass fraction of unburnt gas in those mesh cells which approximate the leading shock wave of the detonation is calculated using all normal and transverse Riemann problems which have an influence on the mesh cell.

3.3. Approximation of a diffracting detonation wave. As a final example, we consider a more interesting and challenging 2D problem, a CJ detonation wave

which is diffracting around a 90 degree corner. We use the reactive Euler equations with the Arrhenius reaction rate law (2.1). For this example the temperature behind the leading shock wave will vary, which causes a change of the reaction rate. We can therefore test our stiff solver as well as the transition between the stiff and the nonstiff approach. Resolved calculations for a similar problem were considered by Xu, Aslam, and Stewart [30] and Aslam and Stewart [1]. The solution of this problem depends strongly on the activation energy and the reaction rate constant. In order to decrease the reaction zone length and make the problem more stiff, we used a larger reaction rate constant than in [30]. We also increased the activation energy in order to obtain the solution structure for our more stiff problem.

The computational domain is $[0, 120] \times [0, 120]$. There is a solid wall in the upper-left corner of the domain for $x \leq 15$ and $y \geq 60$. Initially unburnt gas is in the region $x > 14$. This unburnt state is given by $\rho_u = 1$, $u_u = 0$, $v_u = 0$, and $p_u = 1$. The ratio of specific heat is $\gamma = 1.4$, the heat release is $q_0 = 25$, the activation energy is $E^+ = 35$, and the reaction rate constant is given as $K_0 = 120$. The unburnt state is again connected by a CJ detonation wave to the burnt state, the half-reaction zone length of this CJ detonation wave is about 0.5.

First we consider a resolved approximation using the adaptive mesh refinement algorithm of AMRCLAW [5], [6]. On the finest discretization level, which is used along the leading shock of the detonation wave, the half-reaction zone length is resolved by 16 mesh points. A 3840×3840 grid would be required to achieve this same resolution on a uniform grid. Contour plots of the temperature as well as of the mass fraction of unburnt gas are given in Figure 17.

As the detonation wave moves around the corner, the leading shock weakens, which decreases the temperature behind the shock. When the shock becomes weak enough, it will no longer raise the temperature above the ignition point. Then we get a nonreactive shock traveling vertically followed by a region in which the temperature is high relative to the initial unburnt state but the reaction rate is still negligible. Some distance behind this shock the gas burns via a deflagration wave. This region can be seen in the plot of the temperature; see Figure 17(a).

The shock which is traveling in the horizontal direction is still strong enough to ignite a reaction and remains a CJ detonation wave with the constant speed $s_{CJ} = 7.1247$. At some point along the curved shock front there is a transition between the detonation wave traveling horizontally and the shock-deflagration structure traveling vertically. Our goal in this set of experiments is to demonstrate that on underresolved grids the modified method approximates the correct structure better than the classical fractional step method.

Figures 18–20 show underresolved calculations of this problem. When the shock becomes weaker and the temperature behind the shock becomes lower, the reaction rate behind the shock decreases. In the mesh cells which approximate the leading shock front we will therefore also switch from the stiff to the nonstiff solver. Our modified fractional step scheme, used for the plots on the left-hand side, gives a more accurate approximation of the transition of the solution structure from a detonation wave to a nonreactive shock followed by a deflagration wave. The modified approach on the 120×120 grid (Figure 18(a)) gives a representation of this structure that is at least as good as what is seen with the classical method on the 240×240 grid (Figure 19(b)). The modified scheme on the 240×240 grid gives comparable results as the fractional step scheme on the 480×480 grid (compare Figure 19(a)

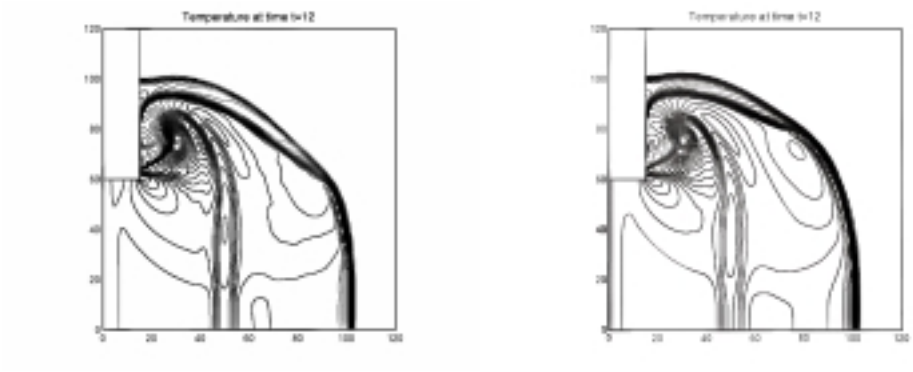

(a) (b)

FIG. 18. *CJ detonation wave diffracting around a corner. Underresolved calculation of the temperature* (120×120 *grid points*). (a) *Using the modified fractional step scheme;* (b) *using the classical fractional step scheme.*

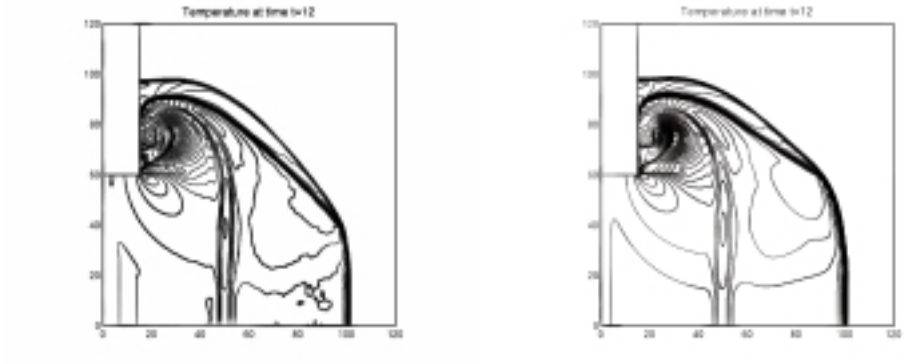

(a) (b)

FIG. 19. *Underresolved calculation of the temperature* (240×240 *grid points*). (a) *Modified fractional step scheme;* (b) *classical fractional step scheme.*

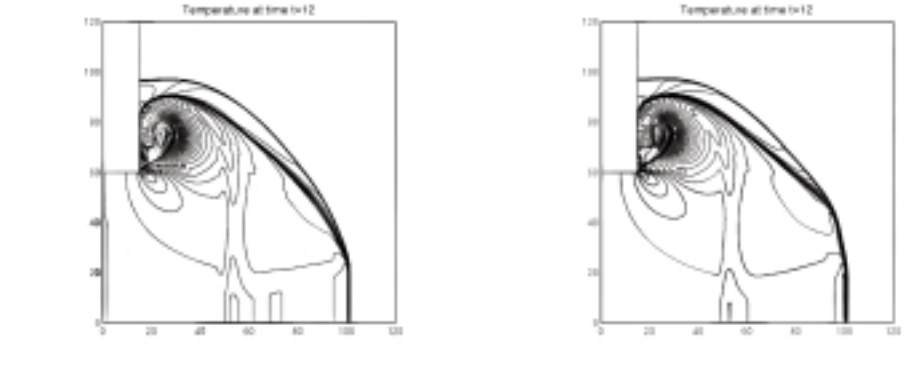

(a) (b)

FIG. 20. *Approximation of the temperature using two grid cells inside the half-reaction zone length* (480×480 *grid points*). (a) *Modified fractional step scheme;* (b) *classical fractional step scheme.*

and Figure 20(b)). Finally the modified scheme on the 480×480 grid produces a very accurate approximation as can be seen by comparing Figure 20(a) with the resolved calculation in Figure 17(a).

For lower or higher values of the activation energy, the point at which the shock structure changes from a reactive to a nonreactive shock moves. If the activation energy is low enough then the shock which is diffracting around the corner may remain strong enough to ignite a reaction and remain a detonation wave everywhere. The reaction rate constant also has an influence on the solution structure. For a larger rate constant the reaction behind the curved shock becomes stronger and the length of the reaction zone becomes smaller. Additional experiments with our method (not shown here) have confirmed that it is robust and yields the correct structure on underresolved grids also in other cases.

4. Conclusions. If stiff source terms are not treated carefully, then the numerical method can produce unphysical solutions even if the scheme is stable. We have considered these numerical difficulties for a combustion problem. If one is not interested in a calculation of the physical processes inside the very small reaction zone but instead wants to determine more global features, e.g., the propagation speed of a detonation wave, then it would be preferable to use a scheme which does not have to resolve the very stiff source term. Here we have shown how the classical fractional step scheme can be modified to give an accurate approximation for the model combustion problem. In section 2 we gave a heuristic motivation of a modification of the fractional step method which was described in that section and extended to 2D problems in section 3.

Our modified fractional step scheme needs information about the structure of the Riemann solution in order to determine the mesh cells over which the leading shock of a detonation wave is smeared. Furthermore, the distance between the shock and contact discontinuity in these mesh cells is required. This information will automatically be provided by an exact Riemann solver as we have described. The distance between the shock and contact discontinuity determines the part of a mesh cell where the source term will be applied in a stiff calculation. For 2D calculations this area depends on all Riemann problems which have an influence to the mesh cell, including the Riemann problems which are solved in order to obtain the fluxes in the transverse direction. However, this further information can be obtained with less effort than the calculation of the change of the cell average due to the solution of the homogeneous problem. Moreover, the modified treatment of the source term is only necessary in those mesh cells which approximate the smeared-out leading shock, e.g., in about three mesh cells for the calculation of the 1D example. Therefore, our modification requires only slightly more effort than the classical fractional step scheme and permits the use of much coarser underresolved grids.

REFERENCES

[1] T.D. Aslam and D.S. Stewart, *Detonation shock dynamics and comparisons with direct numerical simulation*, Combust. Theory Model., 3 (1999), pp. 77–101.

[2] W. Bao and S. Jin, *The Random Projection Method for Stiff Detonation Waves*, Technical Report, School of Mathematics, Georgia Institute of Technology, Atlanta, 1999.

[3] W. Bao and S. Jin, *The Random Projection Method for Hyperbolic Conservation Laws with Stiff Reaction Terms*, Technical Report, School of Mathematics, Georgia Institute of Technology, Atlanta, 1999.

[4] M. Ben-Artzi, *The generalized Riemann problem for reactive flows*, J. Comput. Phys., 81 (1989), pp. 70–101.

[5] M.J. Berger and R.J. LeVeque, amrclaw *software*, http://www.amath.washington.edu/∼rjl/amrclaw/.
[6] M.J. Berger and R.J. LeVeque, *Adaptive mesh refinement using wave-propagation algorithms for hyperbolic systems*, SIAM J. Numer. Anal., 35 (1998), pp. 2298–2316.
[7] A.C. Berkenbosch, *Capturing Detonation Waves for Reactive Euler Equations*, Ph.D. thesis, Technische Universiteit Eindhoven, Eindhoven, The Netherlands, 1995.
[8] A.C. Berkenbosch, E.F. Kaasschieter, and R. Klein, *Detonation capturing for stiff combustion chemistry*, Combust. Theory Model., 2 (1998), pp. 313–348.
[9] A. Bourlioux, *Numerical Study of Unstable Detonations*, Ph.D. thesis, Princeton University, Princeton, NJ, 1991.
[10] A.J. Chorin, *Random choice solution of hyperbolic systems*, J. Comput. Phys., 22 (1976), pp. 517–533.
[11] P. Colella, A. Majda, and V. Roytburd, *Theoretical and numerical structure for reacting shock waves*, SIAM J. Sci. Statist. Comput., 7 (1986), pp. 1059–1080.
[12] R. Courant and K.O. Friedrichs, *Supersonic Flow and Shock Waves*, Springer-Verlag, New York, 1985.
[13] J. Falcovitz and M. Ben-Artzi, *Recent developments of the GRP method*, JSME Internat. J. Ser. B, 38 (1995), pp. 497–517.
[14] J. Glimm, *Solutions in the large for nonlinear hyperbolic systems of equations*, Comm. Pure Appl. Math., 18 (1965), pp. 695–715.
[15] E. Godlewski and P.-A. Raviart, *Numerical Approximation of Hyperbolic Systems of Conservation Laws*, Springer-Verlag, New York, 1995.
[16] R. Jeltsch and P. Klingenstein, *Error estimators for the position of discontinuities in hyperbolic conservation laws with source terms which are solved using operator splitting*, Comput. Visual Sci., 1 (1999), pp. 231–249.
[17] D. Kröner, *Numerical Schemes for Conservation Laws*, Wiley-Teubner, Chichester, Stuttgart, 1997.
[18] R.J. LeVeque, clawpack *software*, http://www.amath.washington.edu/∼rjl/clawpack.html.
[19] R.J. LeVeque, *Numerical Methods for Conservation Laws*, Birkhäuser-Verlag, 1990.
[20] R.J. LeVeque, D. Mihalas, E. Dorfi, and E. Müller, *Computational Methods for Astrophysical Fluid Flow*, Saas-Fee Advanced Course 27 Lecture Notes 1997, O. Steiner and A. Gautschy, eds., Springer-Verlag, Berlin, Heidelberg, 1998.
[21] R.J. LeVeque, *Wave propagation algorithms for multidimensional hyperbolic systems*, J. Comput. Phys., 131 (1997), pp. 327–353.
[22] R.J. LeVeque and K.-M. Shyue, *One-dimensional front tracking based on high resolution wave propagation methods*, SIAM J. Sci. Comput., 16 (1995), pp. 348–377.
[23] R.J. LeVeque and H.C. Yee, *A study of numerical methods for hyperbolic conservation laws with stiff source terms*, J. Comput. Phys., 86 (1990), pp. 187–210.
[24] E.S. Oran and J.P. Boris, *Numerical Simulation of Reactive Flow*, Elsevier, New York, 1987.
[25] R.B. Pember, *Numerical methods for hyperbolic conservation laws with stiff relaxation* I. *Spurious solutions*, SIAM J. Appl. Math., 53 (1993), pp. 1293–1330.
[26] B. Sjögreen and B. Engquist, *Numerical approximation of hyperbolic conservation laws with stiff terms*, in Hyperbolic Problems. Theory, Numerical Methods and Applications, Uppsala, Sweden, Vol. II, 1990, Studentlitteratur, Chartwell-Bratt Ltd., Lund, Sweden, Bromley, UK, 1991, pp. 848–860.
[27] J. Smoller, *Shock Waves and Reaction-Diffusion Equations*, Springer-Verlag, New York, 1994.
[28] V.T. Ton, *Improved shock-capturing methods for multicomponent and reacting flows*, J. Comput. Phys., 128 (1996), pp. 237–253.
[29] B. van Leer, *Towards the ultimate conservative difference scheme* IV. *A new approach to numerical convection*, J. Comput. Phys., 23 (1977), pp. 276–299.
[30] S. Xu, T. Aslam, and D.S. Stewart, *High resolution numerical simulation of ideal and non-ideal compressible reacting flows with embedded internal boundaries*, Combust. Theory Model., 1 (1997), pp. 113–142.